25th ABCM International Congress of Mechanical Engineering
October 20-25, 2019, Uberlândia, MG, Brazil

COB-2019-0249
NUMERICAL AND EXPERIMENTAL COMPARISON OF A HYBRID PV SYSTEM WITH PHASE CHANGING MATERIAL

Maria Cristina Possamai
Willi Gonçalez Osaka
Pontifícia Universidade Católica do Paraná-PUCPR. 1155, Prado Velho – Curitiba
mariacrisp25@outlook.com
willi.osaka@ifpr.edu.br

Luis Mauro Moura
Pontifícia Universidade Católica do Paraná-PUCPR. 1155, Prado Velho – Curitiba
luis.mauro@puc.pr

Stephan Hennings Och
Universidade Federal do Paraná. 1299, Centro – Curitiba
stephan.och@ufpr.br

Abstract
Looking to reduce the amount of greenhouse gases and the use of non-renewable energies in the generation of electricity, this paper has the purpose to evaluate the viability of a glycerin compound behaving as a phase changing material into a hybrid photovoltaic system. Besides that, it compares the results of a theoretical system obtained through simulations in EES software and an indoor prototype containing a solar simulator and a PV cell. The results of the temperature in the numerical system are better than the experimental, showing as the environmental conditions effects on the behavior of the panel. For the voltage, the numerical and experimental system show the same results and the results prove as high temperatures interfere negatively on the efficiency of the PV system.

Keywords: *Photovoltaic, phase change material, efficiency, energy, EES, hybrid PV system.*

1. INTRODUCTION

From the increasing necessity to use clean energy sources in order to reduce non-renewable sources of energy, which emits greenhouse gases causing climate changes, people are looking for increasingly effective ways of transforming solar energy into other energy forms. Another point that leads us to develop equipment for generating energy from the Sun is the fact that planet Earth receives 10,000 times the amount of energy coming from the star than the world consumes in the 21st century (Prado Junior, 2004).

The photovoltaic (PV) cells is one of the most widespread growing technologies in this scenario, however, today its low efficiency of just around 15 % (EKOS,2010) still shows difficulties of economic viability. In addition to the low efficiency of conventional PV systems they have a decrease of 0.4 to 0.5 % efficiency per Kelvin, thus losing efficiency with increasing operating temperature (Ingersoll, 1986) (Krauter et al., 1994). From this problem began the study to find ways to reduce this effect and thus improve the efficiency of the system.

One way to assuage this problem is to use a phase change material (PCM) as part of the system. At the moment that the material reaches its phase change temperature it stays during the changing process in a constant temperature - latent heat. This process slows down the heating of the panel, keeping it at a constant temperature for longer and consequently maintains a better thermal exchange between the PV system and the environment for a longer time. (Ait Hammou and Lacroix, 2006) (Browne, 2015) (Hasan et al., 2010) (Hasan et al., 2004 e2006b).

The purpose of this paper is to compare the results of the temperature and voltage between an experimental of a hybrid solar prototype with phase change material and the theory simulation of this same prototype. Besides that, it shows the feasibility of using a phase change material as a component of the PV system. The material chosen as PCM is a glycerinated base, due to its low melting point near 40 °C.

2. METHODOLOGY

A photovoltaic system consists of a photovoltaic panel and a solar collector, but, it may be improved with other technologies.

In this paper, it is considered for the numerical and experimental prototype a hybrid PV system containing a glycerinated compound acting as a phase change material in a finned chamber, also known as hybrid system with phase change. The hybrid PV module is assembled as shown in Figure 1.

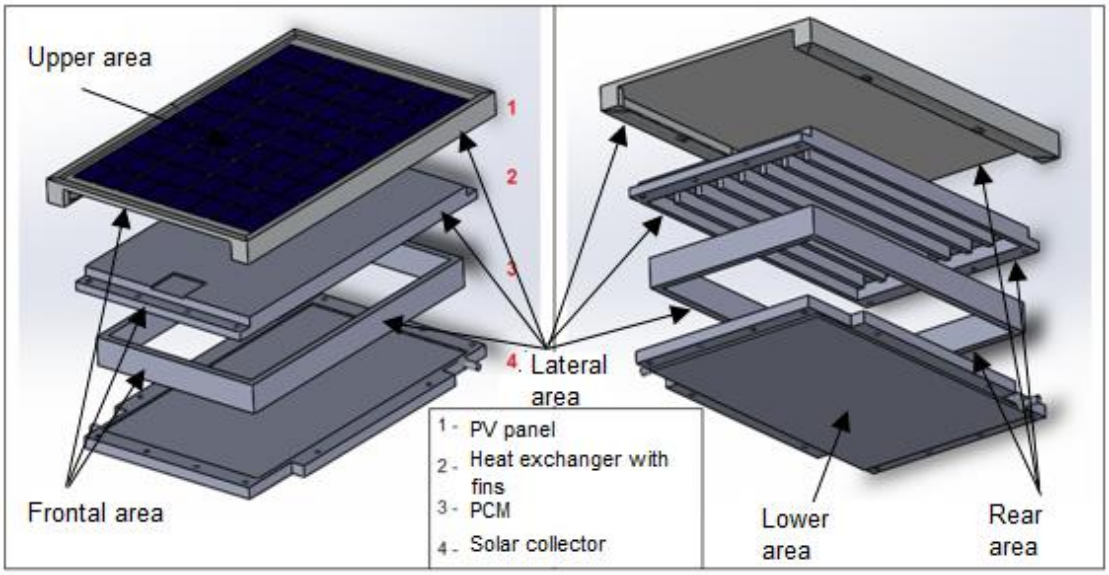

Figure 1: Prototype of the hybrid PV system with changing phase material. From: Osaka W.G., 2017

Table 1 – Parameters of the hybrid PVT system with phase change material used to the equations.

Specific heat of the PV, c_{pv}	700 J/(kg K)
thermal conductivity of the PV, k_{pv}	140 W/(m K)
Efficiency in the CNPT	17 %
FEA	0,89
A	0,092 m^2
A_l	0,0032 m^2
A_{lPCM}	0,00064 m^2
α_{pv}	0,89
L_{al}	0,01 m
L_v	0,005 m
L_{pv}	0,005 m
L_{PCM}	0,002 m
m_{pv}	0,2 kg
m_{M1}	2,2 kg
m_{M2}	0,7 kg
m_{M2}	0,7 kg
m_{water}	10 kg
m_{PCM}	0,15 kg
$m_{PCM,total}$	1,5 kg
c_{water}	4190 J/(kg K)
C_{al}	900 J/(kg K)
Melting temperature of the PCM	40 °C
$K_{PCM,sól}$	0,5 W/(m K)
$K_{PCM,melting}$	0,47 W/(m K)
$K_{PCM,liq}$	0,44 W/(m K)
$C_{PCM,sól}$	2200 J/(kg K)

$c_{PCM,liq}$	1800 J/(kg K)
$cc_{latent\ heat}$	210 J/(kg K)

2.1. Mathematical model:

First of all, it is considered all the PCM in the solid phase. As the system is turned on the heat transfer starts. When the system reaches the temperature of around 40 °C it enters in the process of phase change, passing from the solid phase to the liquid phase, gradually, after that, the PCM is all in the liquid phase. The figure (Figure 2) below represents the PV system considering all the gains and losses of the system:

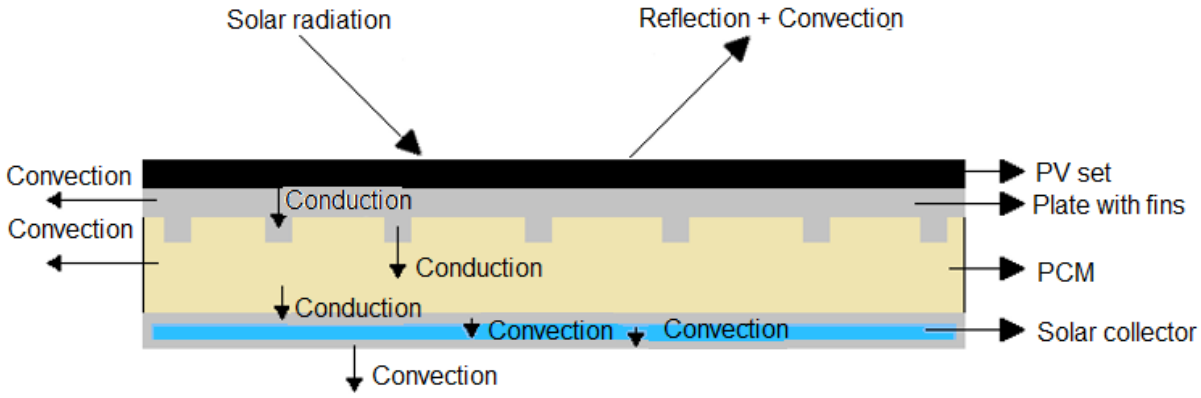

Figure 2: Drawing representing the heat transfers over the system. From: Herculiani L.B. and Possamai M.C., 2017

2.1.1. Numerical Simulation

2.1.1.1. Mathematical considerations:

The simulation of the PV system using PCM is done by the EES software. Since the software is limited, there are many considerations to do during the equation model creation.

For the equation of the mathematical model, it is considered:

- The thermal capacity of the glass located above the photovoltaic panel is neglected;
- The amount of energy exchanged for irradiation between the system and the environment is neglected;
- The heat transfer in the MMF is composed of pure conduction;
- The temperature gradient across the thicknesses of the various layers of system material is non-existent, considering only a mean temperature based on the thermal capacity;
- There is good contact between all the materials used in the system;
- There is no heat exchange between the front and rear areas of the system;
- There is no heat exchange between the solar collector and the environment through the lateral areas.

2.1.1.2. Equations:

After all considerations it uses the energy balance equation to calculate the quantity of energy which the PV panel receives and transfers in the time and the temperature in each component of the system.

The equation of the Balance of energy used for the simulation of the photovoltaic plate with PCM and solar collector is represented by:

$$c_{pv} m_{pv} \frac{dT_{pv}}{dt} = \left[I_{pv}(t)\alpha_{pv} - U_{pv}\left(T_{pv} - T_{amb}\right) - U_{pv,M1} * \left(T_{pv} - T_{M1}\right) - \eta_{pv} q_{pv} \right] \beta A_{pv} \quad (1)$$

The equation 1 represents the amount of energy that the PV panel receives and transfers over time. It is considered that the panel receives heat by irradiation (first term), loses by convection with the environment (second term), conduction with the metallic structure located below the plate (third term) and by its conversion of the energy received into electric energy (fourth term).

In eq. (1) U_{pv} is the overall heat transfer coefficient of the plate to the environment, which is calculated by the following equation:

$$U_{pv} = \left(\frac{1}{hair} + \frac{L_v}{K_v(T)}\right)^{-1} \quad (1.1)$$

The convection coefficient h_{ar} is calculated according to the convection ratio given by (Incropera et al., 2008). First it is needed to analyze whether convection is free or forced through the Reynolds number equation:

$$R_e = \frac{V_{air} L_v}{v} \quad (1.2)$$

For a Reynolds number smaller than $5\ 10^5$ it is concluded that the convection is laminar. The Nusselt equation is used to further calculate the average convection coefficient with air.

$$N_u = 0{,}664 R_e^{\ 1/2} P_r^{\ 1/3} \quad (1.3)$$

From the Nusselt number, the equation 1.4 is used to find the average convection coefficient with air.

$$h_{air} = \frac{N_u K_{air}}{L_v} \quad (1.4)$$

It is used the resistance analysis to determine the overall heat transfer coefficient between the plate and the finned metal U_{pv}.

$$U_{pv,M1} = \left(\frac{L_{pv}}{K_{pv}} + \frac{L_{pt}}{K_{pt}} + \frac{L_{Td}}{K_{Td}} + \frac{L_{al}}{K_{al}(T)}\right)^{-1} \quad (1.5)$$

Finally, the electrical efficiency of a photovoltaic plate can be given by: (Skoplaki and Palyvos, 2009):

$$\eta_{pv} = \eta_0[1 - \beta_0(T_{pv} - T_0)] \quad (2)$$

For the energy balance in the finned aluminum located between the PV plate and the PCM, we have:

$$c_{al} m_{al1} \frac{dT_{al}}{dt} = [U_{pv}(T_{pv} - T_{M1}) - U_{M1,PCM}(T_{M1} - T_{PCM})]A - [h_{air}(T_{M1} - T_{amb})]A_l \quad (3)$$

The equation 3 represents the amount of energy that the aluminum in contact with the PV plate receives and transfers over time. The first term represents the amount received from the PV panel, the second is the amount of heat transferred to the PCM and the third is the amount of heat delivered to the environment by convection through the side areas.

Using the resistance analysis, illustrated in Figure 3, to calculate:

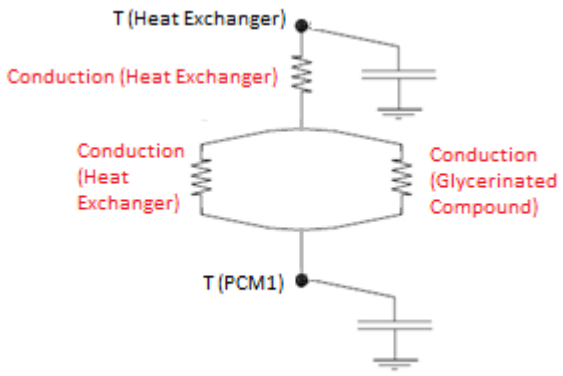

Figure 3: Equivalent resistance model. From: Herculiani L.B. and Possamai M.C., 2017

$$U_{M1,PCM} = \left[\frac{L_{al}}{K_{al}(T)} + \left(\frac{K_{al}(T) A_{p,al}}{L_{al}} + \frac{K_{PCM} A_{p,PCM}}{L_{PCM}}\right)^{-1}\right]^{-1} \quad (3.1)$$

Since the areas of the finned part and the PCM are not the same, each part is multiplied by its respective proportional area. Proportionality is calculated by the occupied area of each part divided by the total.

Because the thickness of the PCM is 30 mm (Malvi et al., 2011) and it has low thermal conductivity, the energy balance of the compound is divided into ten parts of same thermal capacity. Being the first the equation 4:

$$c_{PCM1}m_{PCM1}\frac{dT_{PCM1}}{dt} = \left[U_{M1,PCM1}(T_{M1} - T_{PCM1}) - \frac{K_{PCM}}{L_{PCM}}(T_{PCM1} - T_{PCM2})\right]A - [h_{aIr}(T_{PCM1} - T_{AMB})]A_{lPCM} \quad (4)$$

The above equation represents the amount of energy that the first part of the PCM receives from finned aluminum and transfers over time. The first term of the equation represents the amount of energy received from the finned aluminum, the second is the amount of energy transferred by conduction to the second part of the PCM, and the third term is the amount of heat transferred to the environment by the lateral areas.

For the second to the ninth division of PCM we have:

$$c_{PCMi}m_{PCMi}\frac{dT_{PCMi}}{dt} = \left[\frac{K_{PCM}}{L_{PCM}}\left(T_{PCM[i-1]} - T_{PCM[i]}\right) - \frac{K_{PCM}}{L_{PCM}}\left(T_{PCMi} - T_{PCM[i+1]}\right)\right]A - \left[h_{air}\left(T_{PCM[i]} - T_{AMB}\right)\right]A_{lPCM} \quad (5)$$

For the second to the ninth division of the energy balance equation of the PCM, the first term represents the amount of energy received from the last division of the compound, the second term represents the energy given to the next part of the material and the third term represents the amount of energy lost to the environment, by convection.

For the last division of the PCM we have:

$$c_{PCM10}m_{PCM10}\frac{dT_{PCM10}}{dt} = \left[\frac{K_{PCM}}{L_{PCM}}(T_{PCM9} - T_{PCM10}) - U_{PCM10,M2}(T_{PCM10} - T_{M2})\right]A - [h_{air}(T_{PCM10} - T_{AMB})]A_{lPCM} \quad (6)$$

The PCM temperature equation is completed with the above equation, which describes the energy balance for the last part of the compound. The first term represents the amount of the energy received from the ninth division of the compound. The second term represents the energy given to the upper part of the solar collector, and the third and last term represents the portion of energy given to the environment.

In the last division of the PCM, eq. (6), the overall heat transfer coefficient appears, $U_{MMF3,M2}$, and it can be defined by (Gaur et al., 2017):

$$U_{PCM3,M2} = \left(\frac{K_{PCM}}{L_{PCM}} + \frac{K_{al}}{L_{al}}\right)^{-1} \quad (6.1)$$

To the top of the collector we have the equation of the energy balance:

$$c_{al}m_{al2}\frac{dT_{al}}{dt} = \left[U_{PCM3,M2}(T_{PCM3} - T_{M2}) - h_{water}(T_{M2} - T_{water})\right]A \quad (7)$$

The above equation represents the amount of energy received and transferred by the top of the solar collector over time, where the first term represents the amount of energy received from the PCM and the second, the amount of heat given to water.

For a laminar and completely developed flow in a rectangular chamber, the Nusselt number can be calculated according to the following relation (Jesumathy et al., 2012):

$$N_u = 8{,}235(1 - 1{,}893 \propto +3{,}76 \propto^2 - 5{,}814 \propto^3 + 5{,}316 \propto^4 - 2 \propto^5) \quad (7.1)$$

The $\propto$ is the ratio between the height of the camera and its width:

$$\propto = H_r B_r \quad (7.2)$$

To determine the water convection coefficient, it is used the empirical equation for forced convection (Tiwari, 2004):

$$h_{water} = \frac{K_{water}N_{u,w}}{D_e} \quad (7.3)$$

The D_e, equivalent diameter of a non-circular channel, can be calculated by:

$$D_e = \frac{4H_r B_r}{2(H_r + B_r)} \tag{7.4}$$

The following equation represents the energy balance over time of water in the system. The first term represents the amount of energy received from the top of the solar collector and the second term represents the amount of energy received from the bottom of the solar collector.

$$c_{water} m_{water} \frac{dT_{water}}{dt} = [h_{water}(T_{M2} - T_{water}) - h_{water}(T_{water} - T_{M3})]A \tag{8}$$

The system power balance is completed with the following equation. This represents the energy balance at the bottom of the solar collector, where the first term represents the amount of energy, received by the water, and the second the amount of energy given to the environment through the bottom of the solar collector.

$$c_{al} m_{al3} \frac{dT_{al}}{dt} = [h_{water}(T_{water} - T_{M3}) - h_{ar}(T_{M3} - T_{AMB})]A \tag{9}$$

2.2. Prototype

2.2.1. Development of the Solar Simulator

The prototype simulator is developed within the LST laboratory at PUC-PR. The prototype contains lights that simulate the Sunlight of the environment. For the tests, the simulator has been placed inside a chamber in which humidity and temperature are controlled.

2.2.1.1. Conceptual design and development

The Solar Simulator was built with the following dimensions: 1250 x 1850 x 2100 mm (width x length x height). It follows the size of the commercial PV panels (Figure 4). (Osaka, 2017)

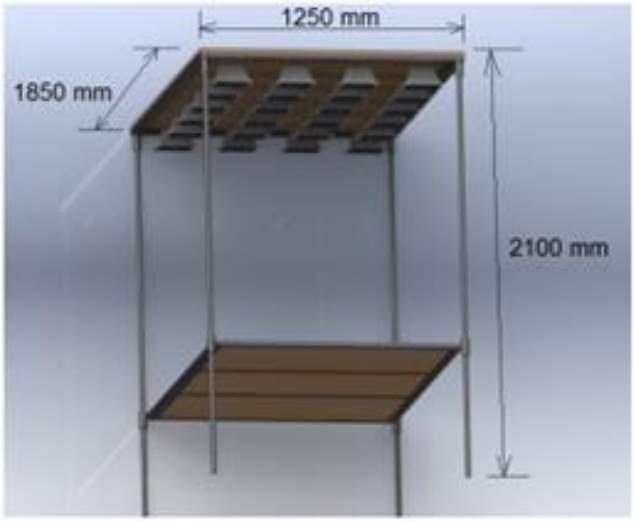

Figure 4: Conceptual design and development of Solar simulator. From: Osaka W.G, 2017

In the Simulator the irradiance is generated by a set of halogen lamps, with rated power of 300 W, arranged in the form of 4 lines of 6 lamps each, totaling 24 lamps. It was opted for this number of bulbs so that there were no large spaces between them, which can generate regions with low irradiance on the surface of the module. Due to the simulator area, around 2.3 m², and the quantity of lamps used, the irradiation was settled to $1000\ Wm^{-2}$.

The lamps were supplied with 220 V voltage to avoid losses by Joule effect on drivers and reduce conductor's oversizing and protective devices (circuit breakers).

In the power supply of the electric circuit, a power controller is installed for PWM (pulse-width modulation) with voltage and maximum power of 220 V-12 kW with control of the lamp power to the irradiance incident on the surface of the module.

The characteristics of the Solar simulator are:
• Dimensions: 3,0 x 3,0 x 3,0 m;
• temperature range: -10 to 65 ° C;
• Humidity range: 10 to 95 %
In the Figure 5 is it possible see the solar simulator assembled inside of the controlled chamber in the LST laboratory.

Figure 5 : Solar simulator instaled in the LST at PUCPR. From: Osaka W.G., 2017

The values of the eletric current and voltage during the time that the simulator works is taken by the Agilent 34970a equipment. For the temperature the equipament used is a thermocouple.

2.2.1.2. Solar panel

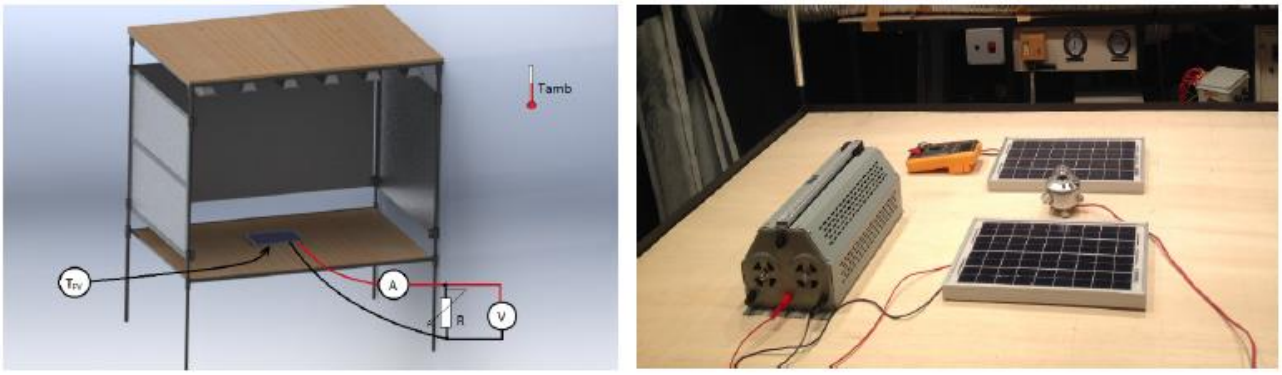

Figure 6: Solar panel inside of the solar simulator. From: Osaka W.G., 2017

When PV module is radiated with halogen lamps, its temperature ranged from the initial 25 ° C to 65 ° C. At each 5 °C increment in the module temperature, the I x V characteristic curve and power are read.

3. RESULTS

After some initial simulations it is possible to analyze that the PV system with material in phase change reaches an efficiency greater than an only hybrid PV system (Fig 7) (Herculiani and Possamai, 2017).

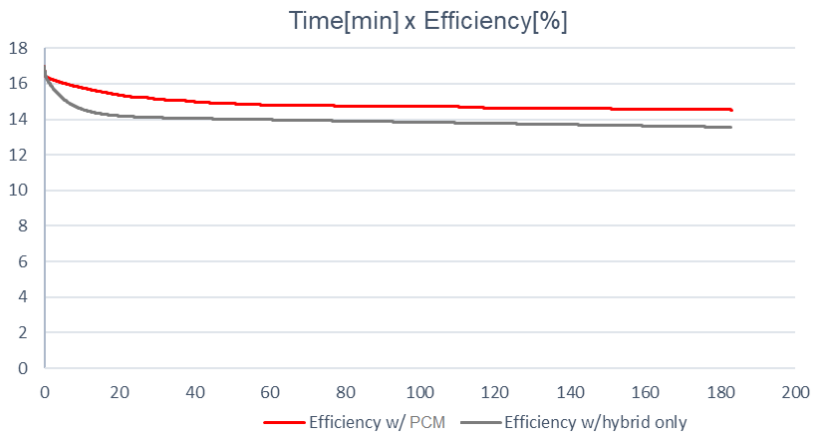

Figure 7: Comparison of the behavior of the efficiencies of each system

The Figure 7 shows that the behavior of the efficiencies in both systems is similar, in which the electric generation efficiencies start at 17 %, since the initial parameters are identical for both systems, and over time decrease. At the end of the simulation, around 180 min, the efficiency of the hybrid phase change material system is 14.5 % and 13.6 % for hybrid only system.

The average efficiency of the hybrid phase change system is 14.9 %, while that of the hybrid system is 13.9 %, accounting for an average efficiency gain of 6.6 %. The biggest difference between efficiencies is in the 14-minute time when the hybrid phase change system has an efficiency gain of 8.7 % over the hybrid system.

This difference in performance between the two systems is due to the fact that the finned heat exchanger assists in heat transfer from the plate. Another point is the temperature stabilization of the glycerin compound during the melting period.

In the Figure 8 there is a comparison between the temperature of the experimental and numerical system.

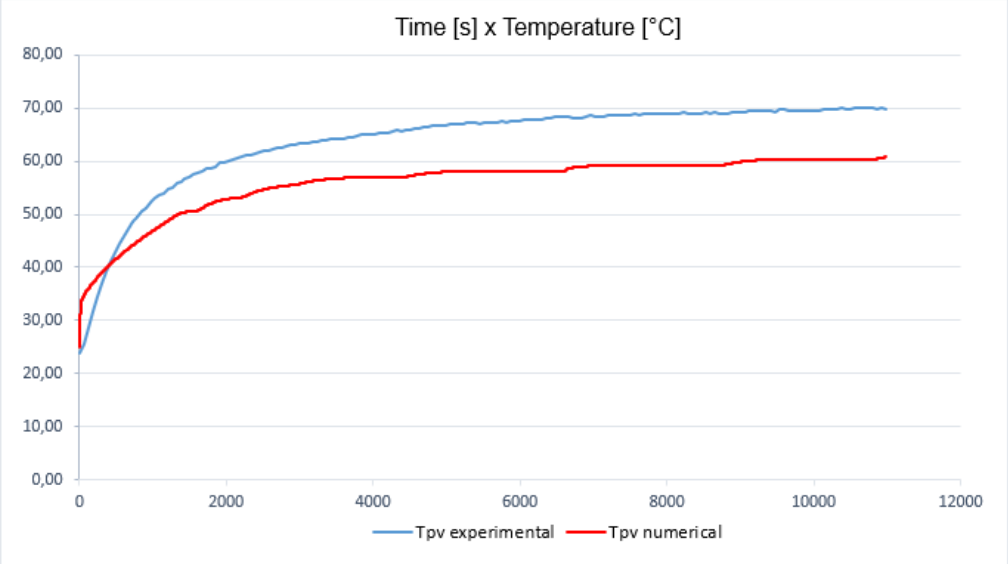

Figure 8: Comparison of the behavior of the temperature during the time for experimental and numerical system.

Both start at 25 °C, but over time the temperature of the numerical system remains more even than the experimental one. This is because in experimental simulation there are environmental contingencies that may interfere with the result. However close to reality one tries to leave the numerical simulation there are factors that we could not predict previously.

The last figure (Figure 9) shows the results of the voltage to electric current for both systems. The voltage remains constant over a long period, but at a certain temperature, the voltage drops, showing that very high panel temperatures negatively affect its performance.

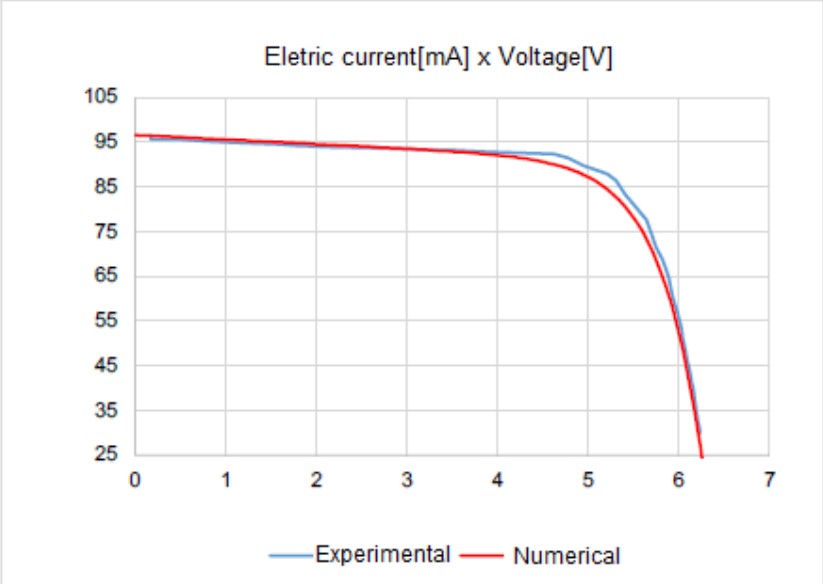

Figure 9: The behavior of the electric current and voltage.

Comparing the experimental and simulated results, we can observe a significant correlation between the results. From this correlation, we conclude that the Solar Simulator has achieved one of its goals, which is to develop an environment for experimentation and evaluation of the electrical efficiency of PV systems in real conditions of temperature, irradiance and ventilation.

4. CONCLUSION

In this paper, it was developed a mathematical model of a hybrid PV system with PCM using the EES software and a prototype in the PUCPR Thermal Systems laboratory. The temperature and voltage results were compared between both situations and the results were satisfactory.

The results obtained in figure 7 demonstrate an efficiency gain in electric power generation using a phase changing material in a finned heat exchanger, enabling the PCM as an alternative in this scenario.

For an improvement of the results, the phase change of the material can be considered gradual in the control volume without the necessity to divide in increments in order to avoid the temperature steps observed in the results. The simulation can also be improved by considering in the equation the amount of energy exchanged through the front and rear areas of the system, as well as the exchange of energy by radiation with the environment.

For the prototype, to get results closer with reality, it is possible assemble the solar panel in an extern environment, where it will consider climatic variations.

5. REFERENCES

Ait Hammou, Z. and Lacroix, M., 2006. « A new PCM storage system for managing simultaneously solar and electric energy". Energy Build. 38 (3) pp. 258-265.

Browne, M.C., Norton, B. and Mc Cormack, S.J., 2015. "Phase change materials for photovoltaic thermal management". Renew. Sustain. Energy Rev. 47 pp. 762-782.

EKOS Brasil, 2010. "Introdução ao Sistema de Aquecimento Solar". 18.

Gaur, A., Ménézo, C. and Giroux–Julien, S., 2017. "Numerical studies on thermal and electrical performance of a fully wetted absorber PVT collector with PCM as a storage medium". Renewable Energy, Volume 109, August pp. 168-187.

Hasan, A., Mccormack, S.J., Huang, M.J. and Norton, B., 2010. "Evaluation of phase change materials for thermal regulation enhancement of building integrated photovoltaics". Sol. Energy 84 pp. 1601-1612.

Herculiani, L.B. and Possamai, M.C., 2017. "Análise numérica de painéis fotovoltaicos híbridos com mudança de fase".

Huang, M.J., Eames, P.C. and Norton, B., 2004. "Thermal regulation of building-integrated photovoltaics using phase change materials". Int. J. Heat Mass Transf. 47 pp. 2715-2733.

Huang, M.J., Eames, P.C. and Norton, B., 2006b. "Phase change materials for limiting temperature rise in building integrated photovoltaics". Sol. Energy 80.

Incropera, F.P., Dewitt, D.P. and Bergman, 2008. T. "Fundamentos de transferência de calor e massa". 6. ed. Rio de Janeiro: LTC.

Ingersoll, J.G., 1986. "Simplified calculation of solar cell temperatures in terrestrial photovoltaic arrays". ASME Journal of Solar Energy Engineering.

Jesumathy, S.P., Udayakumar, M. and Suresh S., 2012. "Heat transfer characteristics in latent heat storage system using paraffin wax". J. Mech. Sci. Technol. 26 (3) pp. 959-965.

Krauter, S., Hanitsch, R. and Wenham, S.R., 1994. "Simulation of thermal and optical performance of PV modules". Renewable Energy.

Malvi, C.S., Dixon – Hardy, D.W. and Crook, R., 2011. "Energy balance model of combined photovoltaic solar-thermal system incorporating phase change material". Solar Energy vol.85

Osaka, W.G., 2017. "Proposta de Sistema fotovoltaico-térmico com material de mudança de fase para a melhoria da eficiência energétic".

Prado Júnior, F.A.A., 2004. "Manual de Engenharia para Sistemas Fotovoltaicos".

Skoplaki, E. and Palyvos, J.A., 2009. "On the temperature dependence of photovoltaic module electrical performance: a review of efficiency/power correlation". Sol. Energy 83 pp. 614-624.

Tiwari, G.N., 2004. Solar Energy: "Fundamentals, Design, Modeling and Applications". Narosa Publishing House.

Nomenclature

A: *Area* m^2
A_l*:Side area* m^2
B_r*: Width of water channel in solar collector* mm
c: Specific heat J kg^{-1} K^{-1}
h: Convection heat transfer coefficient W m^{-2} K^{-1}
H_r*: Height of water channel in solar collector* mm
I: Incident solar radiation W m^{-2}
K: Thermal conductivity W m^{-1} K^{-1}
L: Thickness m
m: Weight kg
PCM: Phase change material
Nu: Nusselt number (Adimensional)
PV: Photovoltaic panel
Re: Reynolds number (Adimensional)
T: Temperature ºC
U: Overall heat transfer coefficient W m^{-2} K^{-1}
V: Velocity m s^{-1}

Greek symbols:
α*: Absorbability (dimensionless)*
ε*: Emissivity (dimensionless)*
β*: FEA (dimensionless)*
η*: efficiency (dimensionless)*
v*: Cinematic vicosity* m^2 s^{-1}

Subscribed:
al: Aluminum
AMB: Environment
air: Environment air
water: Water
PCM: Phase change material
M1: Aluminum finned part
M2: Solar Collector Top
M3: Solar collector bottom
pv: Photovoltaic panel
v: Glass